Journal Name

ARTICLE

Interaction of a Gold(I) Dicarbene Anticancer Drug with Human Telomeric DNA G-Quadruplex: Solution and Computationally Aided X-ray Diffraction Analysis

Received 00th January 20xx,
Accepted 00th January 20xx

DOI: 10.1039/x0xx00000x

www.rsc.org/

Federica Guarra,[a]† Tiziano Marzo,[a,b]† Marta Ferraroni,[c] Francesco Papi,[c] Carla Bazzicalupi,*[c] Paola Gratteri,*[d] Gennaro Pescitelli,[a] Luigi Messori,[b] Tarita Biver[a] and Chiara Gabbiani*[a]

The bis carbene gold(I) complex [Au(1-butyl-3-methyl-2-ylidene)$_2$]PF_6, ([Au(NHC)$_2$]PF_6 hereafter) holds remarkable interest as a perspective anticancer agent. The compound is stable under physiological like conditions: its original structure is retained even in the presence of glutathione (GSH). Previous studies highlighted its high cytotoxicity *in vitro* that correlates with the impairment of crucial metabolic and enzymatic cellular processes (*Magherini et al*, *Oncotarget, 2018, 9, 28042)*. Here, the interaction of [Au(NHC)$_2$]PF_6 with the human telomeric DNA G-quadruplex Tel23 has been investigated in solution by means of high resolution mass spectrometry. ESI MS experiments well document the formation of stable 1:1 adducts between the biscarbene gold complex -in its intact form- and the DNA G-quadruplex. Next, through independent biophysical methods, it is shown that Au(NHC)$_2$]PF_6 binding does not significantly affect the G-quadruplex melting temperature as well as its conformation. The X-ray structure for the [Au(NHC)$_2$]$^+$/Tel24 adduct was eventually obtained by a joint X-ray diffraction and in silico simulation approach. Results clearly evidence the binding requirements of gold ions. Through the careful integration of solution and solid-state data, a quite clear picture emerges for the interaction of this gold complex with the Tel23 G-quadruplex.

Introduction

Among non-platinum antitumor drugs, organometallic compounds with gold in the oxidation states +1 and +3 have recently gained considerable attention, mainly because of their strong cytotoxic effects toward several cancer cell lines.[1] This interest was also driven by the observation that gold compounds usually manifest a very different pharmacological profile compared to established anticancer platinum drugs, implying the occurrence of a alternative molecular mode of action, often not fully understood.[2] In this view, Auranofin *i.e.* [2,3,4,6-tetra-o-acetyl-L-thio-β-D-glyco-pyranosato-S-(triethylphosphine)-gold(I)], a compound currently used in clinic for the treatment of rheumatoid arthritis, represents an instructive example. Several studies have been carried out to elucidate its mechanism of action, indicating the thioredoxin reductase enzyme as one of the likely and most important targets.[2a] This compound is characterized by a remarkable *in vitro* and *in vivo* anticancer activity toward several tumors. Considering these features, Auranofin, represents today the leading compound of the family of medicinal gold complexes and has entered several clinical trials.[3] Following this renewed interest in the gold complexes as possible anticancer agents, a large variety of compounds have been synthesized and characterized for this purpose. Among them, as mentioned above, several organometallic gold (I/III) N-heterocyclic carbene (NHC) complexes were designed and prepared, showing anticancer activity in the micromolar or sub-micromolar range *in vitro*.[4] Despite this wide interest, to date, the exact mode of action of the gold carbene complexes is still largely unclear and several targets -mainly non-genomic- have been suggested. Indeed, the interactions of cytotoxic gold(I) compounds with DNA are generally weaker than those of cisplatin and its analogues, implying the likely occurrence of a substantially different mechanism.[2] Thus, a variety of alternative pathways were hypothesized such as direct mitochondrial damage, proteasome inhibition, modulation of specific kinases or antitelomerase activity. This latter property *i.e.* the ability to inhibit telomerase, has been reported to be -

[a] *Department of Chemistry and Industrial Chemistry, University of Pisa, Via G. Moruzzi 13, 56124 Pisa , Italy. E-mail: chiara.gabbiani@unipi.it.*
[b] *MetMed Lab, Department of Chemistry "U. Schiff", University of Florence, Via della Lastruccia 3, 50019 Sesto Fiorentino, Italy.*
[c] *Department of Chemistry "U. Schiff", University of Florence, Via della Lastruccia 3, 50019 Sesto Fiorentino, Italy. E-mail: carla.bazzicalupi@unifi.it.*
[d] *Department NEUROFARBA – Pharmaceutical and nutraceutical section; Laboratory of Molecular Modeling Cheminformatics & QSAR, University of Firenze, via Ugo Schiff 6, 50019 Sesto Fiorentino, Firenze, Italy. E-mail: paola.gratteri@unifi.it.*
† Equally contributed
Electronic Supplementary Information (ESI) available: [details of any supplementary information available should be included here]. See DOI: 10.1039/x0xx00000x

at least partially- involved in the cytotoxic effects of Auranofin toward selected breast cancer cells.[2d] In view of this, the development of novel molecules with antitelomerase activity represents a very attractive challenge as these properties might be advantageously exploited to design and test novel compounds with improved anticancer profiles.[5] In particular, the capability of metal complexes to interact and stabilize the DNA G-quadruplex can be related to their antitelomerase properties.[6] On the ground of these motivations, the characterisation at the molecular level of the interactions between telomeric G-quadruplex and promising metal-based anticancer drugs is of paramount interest enabling the elucidation of the likely mechanistic aspects involved in the pharmacological effects.[7]

Within this frame, we have selected the dicarbene complex $[Au(NHC)_2]PF_6$, namely bis(1-butyl-3-methyl-imidazole-2-ylidene) gold(I) (figure 1); this is a planar cationic compound previously synthesized and characterized by some of us.[4a] The compound is soluble and stable in physiological-like media (as phosphate buffer, pH 7.4) with no evidence of NHC or chloride detachment even over long observation times (24 h) with full retention of their original structure. A substantial stability was found also in the presence of a large molar excess of biological substrates such as GSH and ascorbic acid (up to 100 fold excess). Noteworthy, when incubated with model proteins bearing solvent exposed sulphur or other coordinating residues, complex does not produces adducts formation.[4a] Notably, the compound showed outstanding cytotoxic properties *in vitro* against several cancer cell lines and it is a potent inhibitor of TrxR activity.[4a,4b,4e] Here we have investigated its interactions with a human telomeric DNA folded into the G-quadruplex in solution and have used a new joint X-ray diffraction and in silico simulation approach to solve the G-quadruplex/$[Au(NHC)_2]^+$ crystal structure.

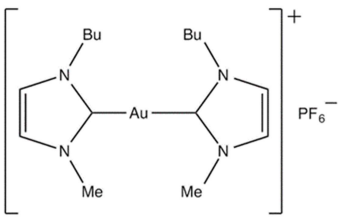

Fig. 1. Chemical structure of the gold(I)-N-heterocyclic carbene complex $[Au(NHC)_2]PF_6$.

Results and Discussion

ESI-MS measurements

The use of electrospray mass spectrometry to characterise the interactions between metal-based drugs and biological targets such as proteins and DNA models, including G-quadruplexes, has been reported to be a powerful investigative strategy.[8] Indeed, this technique has the major advantage to combine a high sensitivity, allowing very low sample consumption, with quick analysis able to provide detailed information on the mode and on the stoichiometry of the occurring interactions. Firstly, an ESI-MS spectrum of the telomere has been recorded to assess the suitability of the experimental procedure. Figure 2 (panel a) shows the obtained spectrum of the Tel23 telomer in which a peak falling at 7380 Da attributable to Tel23 plus five ammonium ions is clearly visible. This finding is relevant being the presence of ammonium ions -that promote the G-quadruplex assembly- the straightforward confirmation that the desired structure is obtained, and is maintained upon MS analysis.[5d] Afterward, Tel23 was incubated with a three -fold excess of $[Au(NHC)_2]PF_6$ for 72 h and the corresponding ESI-MS spectrum recorded. The obtained spectrum is reported in figure 2 (panel b). A peak at 7852 Da assignable to the Tel23 G-quadruplex structure plus the $[Au(NHC)_2]^+$ cation appears. This implies that the complex binds the quadruplex in its entire form with a 1:1 stoichiometry.

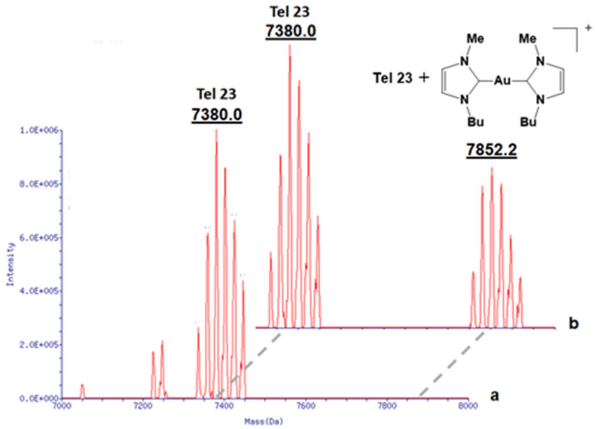

Fig. 2. (a) Deconvoluted ESI-MS spectrum of Tel23 in 50 mM NH4Cl. Concentration of Tel23 was 25 µM in presence of EtOH 60% and 3% of DMSO; (b) deconvoluted ESI-MS spectrum of Tel23 after 72 h incubation with a tree-fold excess of [Au(NHC)2]PF6 in 50 mM NH4Cl (3% of DMSO). Final concentration of Tel23 was 25 µM in presence of EtOH 60%.

Circular dichroism spectroscopy

Circular dichroism spectra are very sensitive to G-quadruplex conformation.[9] As expected for Tel23 G-quadruplex folding in the presence of potassium, the CD spectrum of Tel23 is that typical of an unimolecular G-quadruplex (3+1) hybrid topology with a maximum at ca 286 nm, a shoulder at 268 nm and a minimum at 236 nm (Figure 3).[10] Notably, the addition of 1 to 5 equivalents of $[Au(NHC)_2]PF_6$, did not alter the spectral profile significantly, even after 72h incubation. This finding corroborates the formation of an external adduct with substantial retention of the original G-quadruplex fold.[11] The

hybrid topology of this latter is apparently preserved at high ligand:quadruplex ratios (up to 5:1) whereas similar ligands promote a transition toward a different folding.[5b]

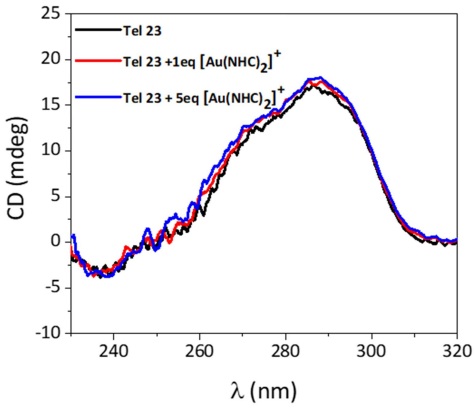

Fig. 3. CD spectra of Tel23 alone (6μM) and in the presence of 1 or 5 equivalents of $[Au(NHC)_2]PF_6$ after 72h incubation in 50 mM potassium phosphate buffer, pH = 7.0, T = 25.0 °C.

UV-Vis thermal denaturation studies

Thermal denaturation studies were then carried out through UV-vis absorption spectroscopy, to assess whether the binding of $[(Au(NHC)_2]PF_6$ to Tel23 affects the stability of the G-quadruplex. The folded oligonucleotide was incubated with various amounts of $[(Au(NHC)_2]PF_6$ for 72h at 37.0 °C in 50 mM potassium phosphate buffer at pH = 7.0. Spectra at increasing temperatures of the samples show an isosbestic point at 279 nm and a relevant decrease of absorbance at 295 nm, typical of G-quadruplexes melting (see the supporting material, figure S0???). Melting temperatures were evaluated as the inflection point of the sigmoidal fit of the experimental trends. In line with the CD results, increasing amounts of $[(Au(NHC)_2]PF_6$ do not significantly influence the stability of the G-quadruplex (Figure 4). This result is different from what observed in the case of a similar caffeinium-based complex/telomeric G4 system, where interaction was quite strong at the same 5/1 ratio. Ref 5B? o Inorg Chem, 2014, 53, 2296-2303?. The reasons for this different behavior will be discussed below.

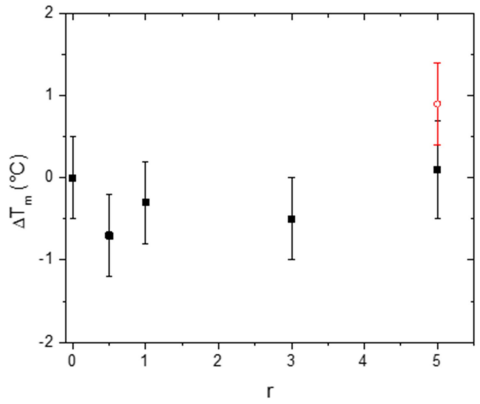

Fig. 4. Variation of melting temperature (T_m) at different molar ratios r=$[Au(NHC)_2]^+$/Tel23. [Tel23] = 1.0 μM (■, 1.0 cm path spectrophotometric cell) or 10 μM (○, 0.1 cm cell), 50 mM potassium phosphate buffer, pH = 7.0. T_m of the telomere alone is 58.7 °C.

Computer aided X-ray crystallography

The crystal structure of the Tel24/$[Au(NHC)_2]^+$ adduct clearly shows monomolecular parallel G-quadruplexes arranged in columns growing along the c axis (figure 5a). The G4 structures are characterized by three stacked G-tetrads (inter-planar distances 3.4 Å) and potassium ions in the internal channel (2.6-3.1 Å apart from the guanine O6 atoms). Symmetry related G4 units stack on one another and form pairs related by two-fold rotation axis. It is likely that the formation of such dimers is favored by the presence of a strontium ion at the interface between couple of adjacent quadruplexes (green in figure 5a). Notably, the used crystallization solution contained only lithium and magnesium cations, while strontium should most likely have been present only as a reagents' impurity. Similar G4 couples were previously reported for several structures, where potassium ions were found in place of the strontium one in our structure.[12]

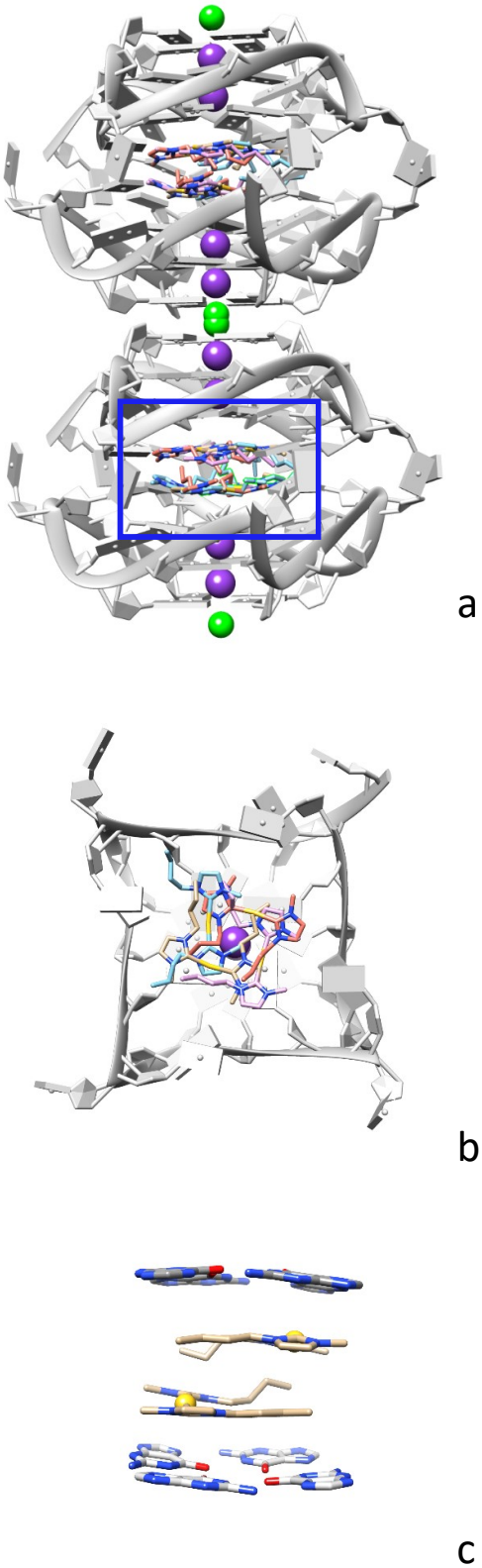

Fig. 5. a) Column of stacked G-quadruplexes in the crystal packing of the Tel24/$[Au(NHC)_2]^+$ crystal structure. Binding site evidenced by a blue line b) Top view of the 3'-end guanine tetrad of the G4 with the stacked disordered $[Au(NHC)_2]^+$ complex, spread over four crystallographic positions. The following color code has been used to identify each single position: salmon (Au1), tan (Au2), light brown (Au3), light pink (Au4), . c) Detail the overall binding site. Only the Au3 complex shown for clarity.(potassium and magnesium ions shown as purple and green spheres, respectively)

The binding site is defined by two-fold symmetry related 3'-end G-tetrads, which lie 11 Å apart from one another. In this cavity, the electron density map shows two symmetry related densities which can account for two drug molecules. Despite the fact that
these densities are not clear, they show the presence of four peaks (eight overall when symmetry is applied), which can be easily associated to four metal atoms lying almost in the same plane, at short distance from one another (longest intermetallic distance 5.7 Å – supporting material Fig. S1). Thus, two gold-complexes, each one spread over four approximately coplanar positions, were supposed to be present in the binding site at inter-planar distances 3.7 Å. It is to be noted that, the residual electron density due to the lighter atoms (C, N) of each ligand didn't allow a clear localization of the overall ligand molecule. As several recent papers remarked the possibility to use theoretical calculations to improve the understanding and interpretation of diffraction data from protein structures,[13] we decided to use high level theoretical calculations to obtain the coordinates for the complex in each of the four positions, and try to refine the complete model against the diffraction data. Thus, we first performed flexible docking procedures followed by optimization at QM/MM level of theory, always constraining the gold atoms to the crystallographic positions, and then we performed final refinements against the diffraction data, without any positional restraints for the complex molecules. Results are shown in Figure 5b and c. In each position, $[Au(NHC)_2]^+$ molecules are found to stack on the external G-tetrads being involved in π-π interactions with two guanines (inter-planar distances 3.5 Å). Despite the slightly different conformations assumed by the butyl chains, the complex was always found in cis conformation. Moreover, three complexes place their alkyl chains just above the tetrad core, occupying it almost completely, while the fourth one is 180° turned along its N-Au-N axis and points its butyl chains outside, towards the region occupied by the loops. Interesting comparisons can be done with respect to the case of the planar Au-dicarbene complex (i.e. $[Au(9\text{-methylcaffein-8-ylidene})_2]^+$) reported in refs 5b and 5d. There, the caffeine units, in combination with a planar structure and the positive charge, ensure high π-π contact surface and, overall, a favourable situation for a strong interaction. Conversely, in our case, replacement of the caffeinium-based ligand with 1-butyl-3-methylimidazolium one, likely leads to a decrease of the π-stacking interaction with the G-quadruplex structure.[5e] Furthermore, the alkyl

chains lying on the tetrad, due to their steric hindrance, may hamper the possibility for a higher stoichiometry ratio of coordination, eventually resulting in a reduced stabilization of G-quadruplex structure compared with [Au(9-methylcaffein-8-ylidene)$_2$]$^+$ ligand.[13d.] The analysis of possible contacts doesn't provide clear information about any favored couple of complexes in the binding site among all the possible combinations. Apparently, any complex in the bottom tetrad can share the binding site with any other complex in the top tetrad. Potential intermetallic distances range from 3.67 Å (Au2…Au4) to 6.88 Å (Au3…Au3). In our opinion, the disorder featuring the binding site could be due to the high degree of freedom featuring the interaction between the guanines tetrad and the small dicarbene complex, which can in any case stack its aromatic rings above two guanines (Fig. 5b). In this case, entropic contributions should be an important driving force for the overall binding, in agreement with both the existence of the complex in solution as well as the difficult localization of the complex's lighter atoms. Nevertheless, the most important information derived from this structure seems to be the electron density for the heavy metal, which is always placed at short distance from the N1 guanine nitrogen (3.5-3.8 Å), clearly recalling what previously reported for the [Au(9-methylcaffein-8-ylidene)$_2$]$^+$ in complex with a 23-mer human telomeric DNA sequence.[5d] In such a structure, all the gold atoms are always sandwiched between two pyrimidine rings, at about 3.5 Å from a pyrimidine nitrogen or carbon atom. This recurrent feature could be an important clue for the understanding of gold carbene complexes' mode of action as well as for the development of new molecules potentially having antitelomerase activity.

Conclusions

In conclusion, we have shown here that the bis carbene gold(I) complex [Au(1-buthyl-3-methyl-2-ylidene)$_2$]PF_6, forms a stable 1:1 adduct with the human telomeric Tel23 G-quadruplex. Adduct formation and the predominance of the 1:1 stoichiometry, are clearly highlighted by mass spectrometry experiments. In addition, mass spectra point out that the interaction is non-covalent in nature, being mostly mediated by electrostatic forces. Notably, the binding of the bis carbene gold(I) complex does not alter the overall conformation of the G-quadruplex fold as shown by the CD spectra. Pairwise, binding of the biscarbene gold(I) complex does not result into any significant alteration of the melting profile of Tel23 quadruplex. The crystal structure of the adduct has been solved by a joint X-ray diffraction and in silico simulation approach. Despite the disorder featuring the binding site, the small dicarbene complex can in any case stack its aromatic rings above two guanines at the time. The gold ions always placed above the guanine residues at short distance from the N1 nitrogen is the most important information derived from this crystal structure, evidencing a recurrent binding feature that could be an important clue for the understanding of the mode of action of gold carbenes. Further efforts will be made in the future in the attempt to study the interaction of the bis carbene gold complex with human telomeric sequences in solution. Through careful integration of solution and solid-state data, a quite clear picture emerges for the interaction of this gold carbene complex with human telomeric DNA revealing the ability of the compound to bind tightly the G-quadruplex structure. Remarkably, this interaction might result into substantial telomerase inhibition, thus contributing to the overall cytotoxic actions of the studied complex, previously documented.

Experimental section

Materials

Tel23 is the human telomeric sequence d[TAG$_3$(TTAGGG)$_3$], purchased from Jena Bioscience. [Au(1-buthyl-3-methyl-2-ylidene)$_2$]PF_6 ([(Au(NHC)$_2$]PF_6) was prepared according to a previously reported procedure.[4a] The lyophilized telomere was dissolved in KCl 50 mM and potassium phosphate 10mM at pH=7.0 to reach a concentration of 1mM. It was then heated to 90° C for 15 min and cooled to RT overnight to allow G-quadruplex formation. [(Au(NHC)$_2$]PF_6 was first dissolved in DMSO to a 5 or 10mM concentration and then diluted in the suitable buffer. Analytical grade reagents and ultra-pure water obtained through a Millipore S.A.670120 Mosheim apparatus were employed.

ESI-MS measurements

The lyophilized telomere was dissolved in 50 mM ammonium chloride to reach a concentration of 1mM and annealed as described above. The G-quadruplex was incubated for 72 h with a 3-fold excess of [(Au(NHC)$_2$]PF_6 in 50 mM ammonium chloride with 3 % DMSO. Before the analysis, the sample was diluted to a final concentration of Tel23 of 25 µM, and EtOH (60 %) was added to optimize and improve signal detection. ESI-MS spectra were recorded by direct injection at 30 µl/min flow rate in an Orbitrap high-resolution mass spectrometer (Thermo, San Jose, CA, USA), equipped with a conventional ESI source. The working conditions were the following: spray voltage 3.1 2 kV, capillary voltage 45 V and capillary temperature 220° C. The sheath and the auxiliary gases were set, respectively, at 17 (arbitrary units) and 1 (arbitrary units). For acquisition, the Xcalibur 2.0 software (Thermo) was used and monoisotopic and average deconvoluted masses were obtained by using the integrated Xtract tool. For spectrum acquisition a nominal resolution (at m/z 400) of 100,000 was used.

UV-Vis thermal denaturation studies

Tel23 1µM was incubated with different amounts of [(Au(NHC)$_2$]PF_6 for 72h at 37.0 °C in 50mM potassium phosphate buffer at pH = 7.0. The samples contain 0.08 % DMSO. UV-vis absorbance spectra of the samples at increasing temperatures from 30°C to 80°C were recorded with a Perkin-Elmer Lambda 35 double ray spectrophotometer, equipped with jacketed cell holders providing a temperature control to within 0.1°C. All spectra were recorded using quartz cuvettes of 1000 µl volume and an optical path of 1.0 cm or 0.1 cm. Thermal denaturation curves were obtained by plotting absorbance at 295 nm vs T °C. Data were analysed using

Origin® 2016 (OriginLab Corp.Northampton, MA, USA) to obtain melting temperatures from the inflexion point of the sigmoid which fits the data plot.

Circular dichroism spectroscopy

CD spectra were recorded (instrument data) with a scan rate of 100 nm/min, a response time of 1 s and a bandwidth of 1 nm. All the spectra were averaged over 4 scans. Cylindrical quartz cuvettes with 1 cm optical path were employed. All measures were carried out in 50 mM potassium phosphate at pH = 7.0 with an amount of DMSO < 0.5 %. First, spectra of 6μM Tel23 G-quadruplex were recorded. Then, spectra of solutions with addition of 1 and 5 equivalents of $[(Au(NHC)_2]PF_6$ were registered over 72h.

Computer aided X-ray Diffraction Analysis

Each lyophilized telomere sequence (Tel12 $d[TAG_3T_2AG_3T]$, Tel23 $d[TAG_3(T_2AG_3)_3]$ or Tel24 $d[TAG_3(T_2AG_3)_3T]$), was dissolved in 20 mM potassium cacodylate pH 6.5 and 50 mM KCl up to a concentration 1 mM, and annealed as described above. The stock DMSO solution of $[(Au(NHC)_2]PF_6$ was added to the DNA annealed solution in 1:1 complex:DNA molar ratio and the resulting solution incubated at 25°C for 20 min. Crystallization trials were set up by mixing 1 μL DNA−drug complex solution to 1 μL crystallization solution. The Tel24/$[Au(NHC)_2]^+$ crystals were obtained at 296 K using the sitting drop vapor diffusion method from a solution containing 20% v/v isopropanol, 50 mM potassium cacodylate pH 6.5, 50 mM Li_2SO_4, 50 mM $MgSO_4$, on the basis of a reported screening.(Campbell, N. H.; Parkinson, G. N. Methods 2007, 43, 252−263) Drops were equilibrated against the same solution (100 μL).

The crystal of the Tel24/$[Au(NHC)_2]^+$ complex belonged to the space group C2 (5 - monoclinic system) with cell dimensions a = 36.60 Å, b = 71.37 Å, c = 27.05 Å, β = 92.42°. Data collection on crystals of the DNA−drug complex was performed at 100 K, using as cryoprotectant a 30% v/v glycerol aqueous solution, and the synchrotron radiation (λ = 0.872900 Å, gold L-I X-ray absorption edge) at the ID23-2 Beamline, ESRF Grenoble. Data were integrated and scaled using the program XDS.[14] The structure was solved by the Molecular Replacement technique using the program MOLREP[15] and the coordinates of the Tel23 G-quadruplex structure (PDB code 3R6R),[16] without all the heteroatoms, as a search model. The model was refined with the program Refmac5[17] from the CCP4 program suite.[18] Manual rebuilding of the model was performed using the program Coot.[19] The model obtained at this step of refinement consisted of the overall DNA coordinates, the cocrystallized waters, potassium and strontium ions, and a gold ion, spread over four sites (0.25 occupancy factor each). The gold positions were also verified from the anomalous Fourier difference map. The 25 % electron density from the lighter atoms of each ligand was too low to be clearly observed in the maps, so making the molecule positioning arbitrary.

In silico calculations were carried out with the purpose to find the most probable ligand positions in the Tel24/$[Au(NHC)_2]^+$ adduct. The starting coordinates for the metal complex in cis conformation (both butyl groups on the same side) were obtained from the crystal structure of [Au(bis(1-butyl-3-methyl-imidazole-2-ylidene)]PF6 (CCDC code 936581),[4a] while the trans conformer was obtained from the cis one by proper modification. Both cis and trans conformations were quantum mechanically optimized at the B3LYP/LACV3P**+ level of theory[20] and the atomic electrostatic charges were calculated and used in the following steps. The crystallographic coordinates of the Tel24 G-quadruplex were used as a frozen target in all the steps. The ligand was flexibly docked on the target restraining the gold atom positions to the crystallographic coordinates. One by one, all the four gold positions close to the same G-tetrad were considered for the calculations. The resulting adducts were then optimized by QM/MM approach, always constraining the gold atoms to the crystallographic positions ((QSite, version 9.9, Schroedinger, LLC, New York, NY, 2016) ligand: DFT B3LYP, LACVP basis set;[20] DNA: OPLS2005,[21] all DNA residues frozen at the crystallographic coordinates). The four lowest energy structures, one per gold ion (indicated in the following as Au1, Au2, Au3 and Au4), were selected, added together and refined to the final Rfactor = 22.8 % and Rfree factor = 25.5% (2.0 Å resolution). Occupancy factors were set 0 for all butyl carbon atoms (Au2) lying outside the visible electron density. Data collection and refinement statistics are reported in Table S1, Supporting Information. Final coordinates and structure factors have been deposited with the Protein Data Bank (PDB accession number 6H5R).

Conflicts of interest

There are no conflicts to declare.

Acknowledgements

We gratefully acknowledge Beneficentia Stiftung, ITT (Istituto Toscano Tumori), Ente Cassa Risparmio Firenze (ECR) for a grant to FP and AIRC for funding the projects (IG-16049) COST Action CM1105 and University of Pisa (PRA_2017_25, to C.G. and T.M.) are also acknowledged. T.M. thanks AIRC-FIRC (Fondazione Italiana per la Ricerca sul Cancro) for the 3-years Fellowship for Italy, Project Code: 18044. CIRCMSB and CISM (University of Florence) are also acknowledged. CHECK giustificazione

Notes and references

1 a) S. Nobili, E. Mini, I. Landini, C. Gabbiani, A. Casini, L. Messori, *Med. Res. Rev.* 2010, **30**, 550–580; b) W. Liu, R. Gust, *Coord. Chem. Rev.* 2016, **329**, 191–213.

2 a) I. Ott, Coord. Chem. Rev. 2009, *253*, 1670-1681; b) A. Casini, L. Messori, *Curr. Top. Med. Chem.* 2011, *11*, 2647-2660; c) L. Oehninger, R. Rubbiani, I. Ott, *Dalton Trans.* 2013, **42**, 3269-3284; d) N.H. Kim, H. J. Park, M.K. Oh, I.S. Kim, *BMB Rep.* 2013, **46**, 59-64.

3 https://clinicaltrials.gov/ct2/results?cond=auranofin

4 a) L. Messori, L. Marchetti, L. Massai, F. Scaletti, A. Guerri, I. Landini, S. Nobili, G. Perrone, E. Mini, P. Leoni, M. Pasquali, C. Gabbiani, *Inorg. Chem.* 2014, **53**, 2396–403; b) N. Estrada-Ortiz, F. Guarra, I. A. M. de Graaf, L. Marchetti, M. H. de Jager, G. M. M. Groothuis, C. Gabbiani, A. Casini, *ChemMedChem* 2017, **12**, 1429–35; c) Ö. Karaca, V. Scalcon, S.M. Meier-Menches, R. Bonsignore, J.M.J.L Brouwer, F. Tonolo, A. Folda, M.P. Rigobello, F.E. Kühn, A. Casini, *Inorg. Chem.* 2017, **56**, 14237-14250; d) C. Schmidt, B. Karge, R. Misgeld, A. Prokop, R. Franke, M. Brönstrup, I. Ott, *Chem. Eur. J.* 2017, **23**, 1869 – 1880, e) F. Magherini, T. Fiaschi, E. Valocchia, M. Becatti, A. Pratesi, T. Marzo, L. Massai, C. Gabbiani, I. Landini, S. Nobili, E. Mini, L. Messori, A. Modesti, T. Gamberi, *Oncotarget*, 2018, **9**, 28042.

5 a) B. Maji, S. Bhattacharya, *Chem. Commun*. 2014, **50**, 6422-38; b) F. Papi, C. Bazzicalupi, M. Ferraroni, L. Massai, B. Bertrand, P. Gratteri, D. Colangelo, L. Messori, *Chem. Eur. J.* 2017, **23**, 13784–13791; c) Q. Cao, Y. Li, E. Freisinger, P. Z. Qin, R. K. O. Sigel, Z.-W. Mao, Inorg. Chem. Front., 2017, **4**, 10-32; d) C. Bazzicalupi, M. Ferraroni, F. Papi, L. Massai, B. Bertrand, L. Messori, P. Gratteri, A. Casini, *Angew. Chem. Int. Ed.* 2016, **55**, 4256 –4259; e) D. Wragg, A. de Almeida, R. Bonsignore, F. E. Kuhn, S. Leoni, A. Casini, *Angew. Chem. Int. Ed*. 2018, **57**, 1 – 6.

6 B. Maji, S. Bhattachary, *Chem. Commun.*, 2014, **50**, 6422-3648.

7 a) T. Che, S.-B. Chen, J.-L Tu, B. Wang, Y.-Q. Wang, Y. Zhang, J. Wang, Z.-Q. Wang, Z.-P. Zhang, T.-M. Ou, Y. Zhao, J.-H. Tan, Z.-S. Huang, *J. Med. Chem.* 2018, **61**, 3436−3453; b) Blasiak J., *Curr. Med. Chem.* 2017, **24**, 1488-1503; c) Q. Cao, Y. Li, E. Freisinger, P. Z. Qin, R. K. O. Sigel, Z.-Wan Mao, *Inorg. Chem. Front.* 2017, **4**, 10-32; d) M.K. Islam, P.J. Jackson, K.M. Rahman, D.E. Thurston, *Future Med. Chem.*, 2016, **8**, 1259-1290.

8 a) A. Merlino, T. Marzo, L. Messori, *Chem. Eur. J.* 2017, **23**, 6942-6947; b) T. Marzo, D. Cirri, C. Gabbiani, T. Gamberi, F. Magherini, A. Pratesi, A. Guerri, T. Biver, F. Binacchi, M. Stefanini, A. Arcangeli, L. Messori, *ACS Med. Chem. Lett.* 2017, **8**, 997-1001; c) C. Martín-Santos, E. Michelucci, T. Marzo, L. Messori, P. Szumlas, P.J. Bednarski, R. Mas-Ballesté, C. Navarro-Ranninger, S. Cabrera, J. Alemán, *J. Inorg. Biochem.* 2015, **153**, 339-345; d) L. Messori, T. Marzo, C. Gabbiani, A.A. Valdes, A.G. Quiroga, A. Merlino, *Inorg. Chem.* 2013, **52**, 13827-13829; e) P. Gratteri, L. Massai, E. Michelucci, R. Rigo, L. Messori, M. A. Cinellu, C. Musetti, C. Sissi, C. Bazzicalupi, *Dalton Trans*. 2015, **44**, 3633-3639.

9 R. del Villar-Guerra, J.O. Trent, J.B. Chaires, *Angew. Chem. Int. Ed. Engl.* 2018, **57**, 7171-7175.

10 K.N. Luu, A.T. Phan, V. Kuryavyi, L. Lacroix, D.J. Patel, *J. Am. Chem. Soc.* 2006, **128**, 9963–9970.

11 a) N. Nagesh, R. Buscaglia, J.M. Dettler, E.A. Lewis, *Biophys. J.* 2010, **98**, 2628–2633; b) F.S. Di Leva, P. Zizza, C. Cingolani, C. D'Angelo, B. Pagano, J. Amato, E. Salvati, C. Sissi, O. Pinato, L. Marinelli, A. Cavalli, S. Cosconati, E. Novellino, A. Randazzo, A. Biroccio, *J. Med. Chem.* 2013, **56**, 9646−9654.

12 a) G.N. Parkinson, M.P. Lee, S. Neidle, *Nature* 2002, **417**, 876-880; b) G.N. Parkinson, R. Ghosh, S. Neidle, *Biochemistry*, 2007, **46**, 2390-2397; c) G.N. Parkinson, F. Cuenca, S. Neidle, *J. Mol. Biol.* 2008, **381**, 1145-1156; d) N.H. Campbell, N.H. Karim, G.N. Parkinson, M. Gunaratnam, V. Petrucci, A.K. Todd, R. Vilar, S. Neidle, *J. Med. Chem.* 2012, **55**, 209-222; e) M. Micco, G.W. Collie, A.G. Dale, S.A. Ohnmacht, I. Pazitna, M. Gunaratnam, A.P. Reszka, S. Neidle, *J. Med. Chem.* 2013, **56**, 2959-2974; f) G.W. Collie, R. Promontorio, S.M. Hampel, M. Micco, S. Neidle, G.N. Parkinson, *J. Am. Chem. Soc.*, 2012, **134**, 2723-2731; g) J.M., Nicoludis, S.T. Miller, P.D. Jeffrey, S.P. Barrett, P.R. Rablen, T.J. Lawton, L.A. Yatsunyk, J. Am. Chem. Soc. 2012, **134**, 20446-20456; h) I. Russo Krauss, S. Ramaswamy, S. Neidle, S. Haider, G.N. Parkinson, *J. Am. Chem. Soc.* 2016, **138**, 1226-1233.

13 a) L. Cao, O. Caldararu, U. Ryde, *J. Phys. Chem. B* 2017, **121**, 8242−8262; b) M. Zheng, N.W. Moriarty, Y. Xu, J.R. Reimers, P.V. Afoninea, M.P. Waller, *Acta Cryst.* 2017. **D73**, 1020–1028; c) L. Cao, O. Caldararu, A.C. Rosenzweig, U. Ryde, *Angew. Chem. Int. Ed.* 2018, **57**, 162-166; d) A. Nocentini, F. Carta, M. Tanc, S. Selleri, C.T. Supuran, C. Bazzicalupi, P. Gratteri *Chem. Eur. J.* 2018, **24**, 7840 – 7844; *F. Papi,* C. Bazzicalupi, M. Ferraroni, L. Massai, B. Bertrand, P. Gratteri, D. Colangelo, L. Messori *Chem. Eur. J.* 2017, **23**,13784 –13791.

14 W. Kabsch, *Acta Crystallogr. Sect. D: Biol. Crystallogr.* 2010, **D66**, 125−132.

15 A. Vagin, A. Teplyakov, *J. Appl. Cryst.* 1997, **30**, 1022–1025.

16 C. Bazzicalupi, M. Ferraroni, A.R. Bilia, F. Scheggi, P. Gratteri, *Nucleic Acids Res.* 2013, **41**, 632-638.

17 G.N. Murshudov, P. Skubák, A.A. Lebedev, N.S. Pannu, R.A. Steiner, R.A. Nicholls, M.D. Winn, F. Long, A.A. Vagin, *Acta Crystallogr., Sect. D: Biol. Crystallogr.* 2011, **D67**, 355−367.

18 M.D. Winn, C.C. Ballard, K.D. Cowtan, E.J. Dodson, P. Emsley, P.R. Evans, R.M. Keegan, E.B. Krissinel, A.G.W. Leslie, A. McCoy, S.J. McNicholas, G.N. Murshudov, N.S. Pannu, E.A. Potterton, H.R. Powell, R.J. Read, A.A. Vagin, K.S. Wilson, *Acta Crystallogr., Sect. D: Biol. Crystallogr.* 2011, **D67**, 235−242.

19 P. Emsley, B. Lohkamp, W.G. Scott, K. Cowtan, *Acta Crystallogr., Sect. D: Biol. Crystallogr.* 2010, **D66**, 486−501.

20 a) A.D. Becke, *J. Chem. Phys*. 1993, **98**, 1372–1380; b) A.D. Becke, J. *Chem. Phys.* 1993, **98**, 5648–5657; c) C. Lee, W. Yang, R. G. Parr, *Phys. Rev. B* 1988, **37**, 785-780; d) B. Miehlich, A. Savin, H. Stoll, H. Preuss, *Chem. Phys. Lett.* 1989, **157**, 200–208; e) P.J. Hay, W.R. Wadt, *J. Chem. Phys.* 1985, **82**, 299–308.

21 a) G.A. Kaminski, R.A. Friesner, J. Tirado-Rives, W.L.J. Jorgensen, J. *Phys. Chem. B* 2001, **105**, 6474−6487; b) V. Hornak, R. Abel, A. Okur, B. Strockbine, A. Roitberg, C. Simmerling, *Proteins: Struct., Funct., Genet.* 2006, **65**, 712−725.